

PHOTO- AND HADRO-PRODUCTION OF η' MESON¹K. Nakayama^{2*}, H. Haberzettl^{3†}^{*}Department of Physics and Astronomy, University of Georgia, Athens, GA 30602, USA.[†]Department of Physics, The George Washington University, Washington, DC 20052, USA.

Received 3 November 2005, in final form 29 November 2005, accepted 12 December 2005

A combined analysis of the existing data on the reactions $\gamma p \rightarrow p\eta'$ and $pp \rightarrow pp\eta'$, based on a relativistic meson exchange model of hadronic interactions, is presented.

PACS: 25.20.Lj, 13.60.Le, 13.75.-n, 14.20.Gk

1 Introduction

One of the primary interests in investigating η' meson-production reactions is that they may be suited to extract information on nucleon resonances, N^* , in the less explored higher N^* mass region. Current knowledge of most of the nucleon resonances is mainly due to the study of πN scattering and/or pion photoproduction off the nucleon. Since the η' meson is much heavier than a pion, η' meson-production processes near threshold necessarily sample a much higher resonance-mass region than the corresponding pion production processes. Therefore, they are well-suited for investigating high-mass resonances in low partial-wave states. Furthermore, these reactions provide opportunities to study those resonances that couple only weakly to pions, in particular, those referred to as “missing resonances”. In the particular case of the $NN \rightarrow NN\eta'$ reaction, it offers a unique opportunity to study the excitation mechanism of those resonances.

Another special interest in η' photoproduction is the possibility to impose a more stringent constraint on its yet poorly known coupling strength to the nucleon. This has attracted much attention in connection with the so-called “nucleon-spin crisis” in polarized deep inelastic lepton scattering [1] in that the $NN\eta'$ coupling constant can be related to the quark contribution to the “spin” of the nucleon [2]. Reaction processes where the η' meson is produced directly off a nucleon may offer a unique opportunity to extract this coupling constant.

The major purpose of the present work is to perform a combined analysis of the $\gamma p \rightarrow p\eta'$ and $pp \rightarrow pp\eta'$ reactions within a relativistic meson-exchange model of hadronic interactions. The photoproduction reaction is described in the tree-level approximation, where a phenomenological contact term is introduced in order to guarantee the gauge invariant condition of the full amplitude. The latter consists of nucleonic, mesonic and (nucleon) resonance currents as depicted in

¹Presented at the Workshop on Production and Decay of η and η' Mesons (ETA05), Cracow, 15–18 September 2005.²E-mail address: nakayama@uga.edu³E-mail address: helmut@gwu.edu

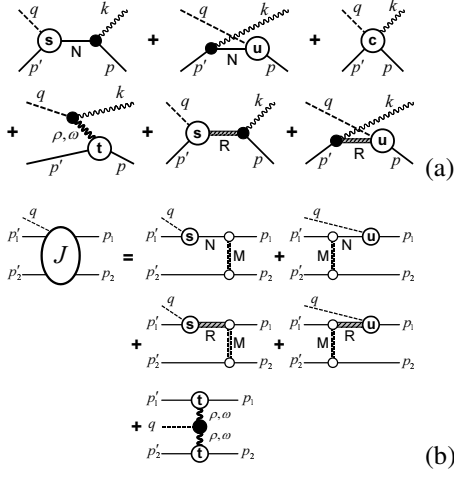


Fig. 1. (a): Diagrams contributing to $\gamma p \rightarrow \eta' p$. The intermediate baryon states are denoted N for the nucleon, and R for the nucleon resonances. The total current is made gauge-invariant by an appropriate choice of the contact current depicted in the top-right diagram. The nucleonic current (nuc) referred to in the text corresponds to the top line of diagrams; the mesonic current (mec) and resonance current contributions correspond, respectively, to the leftmost diagram and the two diagrams on the right of the bottom line of diagrams. (b): Basic production current for $pp \rightarrow pp\eta'$. M incorporates all exchanges of mesons $\pi, \eta, \rho, \omega, \sigma,$ and $a_0 (\equiv \delta)$ for the nucleon graphs and $\pi, \rho,$ and ω for the resonance graphs.

Fig. 1a. The hadro-production reaction is described in the Distorted Wave Born Approximation (DWBA) where both the initial and final state (NN) interactions are taken into account. Here, the production current (see Fig. 1b) is derived consistently with the production current used in the photoproduction reaction. Further details can be found in ref. [3].

2 Analysis of the SAPHIR data on $\gamma p \rightarrow p\eta'$

The objectives of analyzing the SAPHIR data [8] on η' photoproduction are:

- 1) To shed light on the conflicting conclusions of the existing model calculations for these data. These contradictions are: a) The origin of the shape of the observed angular distribution. Zhao [4] has emphasized that this is due to the interference among the resonance currents, while Chiang et al. [5] have concluded that it is due to the interference between the resonance and t-channel mesonic currents. Yet, Sibirtsev et al. [6] have claimed that the mesonic current is responsible for the observed angular distribution. The latter authors use a t-dependent exponential form factor in their mesonic current. b) t-channel meson-exchange versus Regge trajectory. Chiang et al. [5] have emphasized that the SAPHIR data can be described only if the Regge trajectory is used in the t-channel mesonic current, while other authors [6, 7] have used ordinary vector meson exchanges.
- 2) Can we constrain the $NN\eta'$ coupling constant from the photoproduction reaction?
- 3) To which extent are we able to identify the nucleon resonances from the differential cross section data, i.e., can, e.g., the mass of the resonance be pinned down from the existing cross section data?
- 4) Provide inputs for the $NN \rightarrow NN\eta'$ reaction.

Our results for the angular distribution at various energies are shown in Fig. 2, together with the SAPHIR data [8]. First of all, the mesonic current is responsible for the measured forward

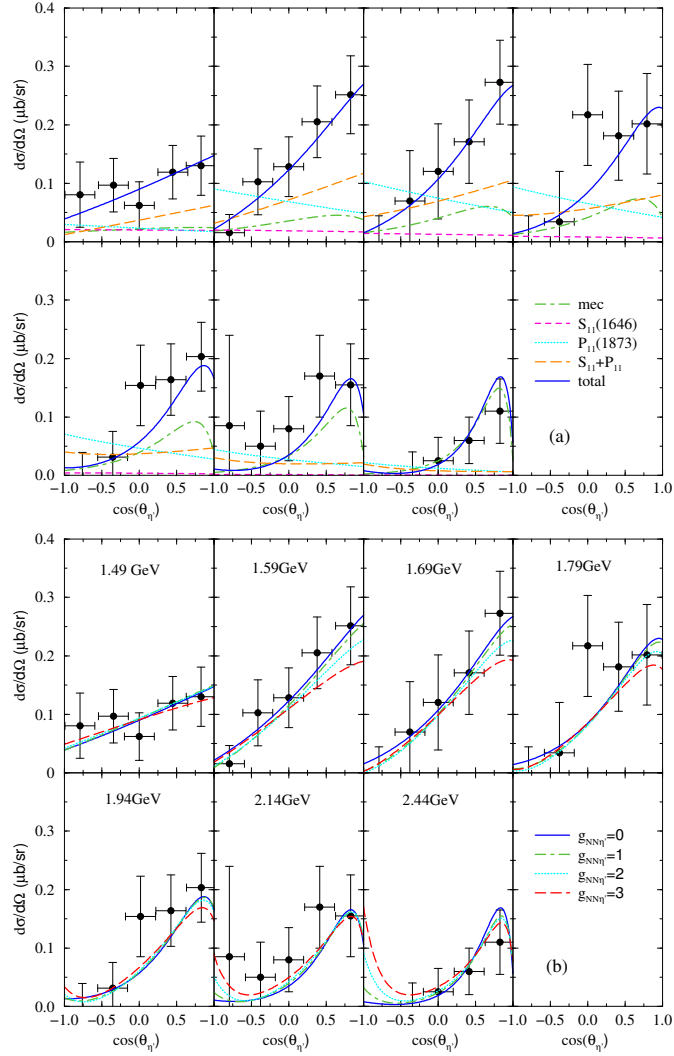


Fig. 2. Differential cross section for $\gamma p \rightarrow p\eta'$ according to the mechanisms shown in Fig. 1a. Panel (a) includes the meson-exchange current (mec), the S_{11} and P_{11} resonances. In (b), successively stronger (as indicated by the values of the $g_{NN\eta'}$ coupling constant) nucleonic current (nuc) contributions are added to the results shown in panel (a). In each case, the model parameters are determined by best fits. The meaning of the corresponding lines is indicated in the panels. The data are from Ref. [8].

peaked angular shape at higher energies. The P_{11} resonance contribution is much larger than that due to the S_{11} resonance. Also, note the interference effects among different currents; the P_{11} resonance gives rise to a larger backward angle cross sections, while the total resonance current, $S_{11} + P_{11}$, yields a larger forward angle cross sections. Adding the mesonic current

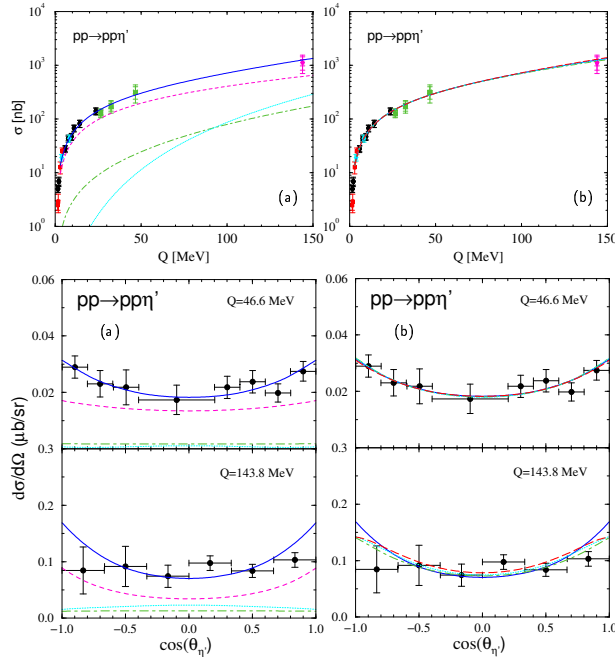


Fig. 3. Excess energy, Q , dependence of the total cross section (top row) and angular distributions at $Q = 46.6$ and 143.8 MeV in the c.m. frame of the system (bottom row) for $pp \rightarrow pp\eta'$, according to the mechanisms depicted in Fig. 1b. The panels labeled (a) and (b) in both rows correspond to the respective panels (a) and (b) in Fig. 2, and all line styles are explained there. In part (b) of the total cross section and in the corresponding 47-MeV angular distribution, on the present scales, all curves practically lie on top of each other, i.e., these results are very insensitive to the nucleonic contributions. The data are from refs. [9, 10].

leads to a further enhancement of the forward cross sections. We mention that the inclusion of the mesonic and S_{11} resonance currents only is not sufficient to describe the strong angular dependence at lower energies [3]. Also, the nucleonic current, through its interference with the mesonic and S_{11} resonance currents, makes the angular distribution more pronounced [3] but not as pronounced as the addition of the P_{11} resonance shown in Fig. 2a. It is, therefore, clear that the observed angular distribution is a result of the rather non-trivial interference among different currents.

Fig. 2b displays our results for various values of the $NN\eta'$ coupling constant, $g_{NN\eta'}$, in the nucleonic current. Here, we also include the mesonic, S_{11} and P_{11} resonance currents. Note that the nucleonic current becomes pronounced at backward angles as the energy increases which is due to the u-channel diagram. We see that $g_{NN\eta'}$ cannot be much larger than 3. Naively, we would expect that more accurate data at higher energies will enable us to reduce this upper limit. See, however, the analysis of the high-precision CLAS data in Section 4.

Next we address the issue of the ordinary meson-exchange versus Regge trajectory in the t-channel mesonic current. The mesonic current based on the ordinary vector-meson exchange contains an extra form factor at the electromagnetic vertex, while that based on the Regge trajectory contains no such form factor. We verified that both models describe the data equally well, although there are some differences in detail. However, one important point to be notice here is that the resulting resonance parameters are quite different. This is quite disturbing, for it reveals a clear model dependence in the extracted resonance parameters. Further investigation of this important issue is required in future works.

We have also verified the sensitivity/insensitivity of the differential cross section data to the mass value of the nucleon resonance. In particular, we found that the results with the S_{11} mass values which differ by about 100 MeV are hardly distinguishable from each other in the differential cross sections. This gives a rough idea about the uncertainty one should expect on the extracted resonance mass values based only on the differential cross section data.

3 Analysis of the $pp \rightarrow pp\eta'$ reaction

The production current for this reaction is obtained from the photoproduction current by replacing the photon by a relevant meson M and attaching the nucleon to it (see Fig. 1b). In this way, the only free parameter is the coupling constant at the nucleon-resonance transition vertex which is adjusted to reproduce the available data from SATURNE [9] and COSY [10]. The results are shown in Fig. 3. We see that the data are well reproduced overall. Unlike the case of photoproduction where the P_{11} resonance contribution was much larger than that of S_{11} resonance, here, the S_{11} resonance is, by far, the dominant current in the entire energy region considered which is due to the rather flat angular distributions exhibited by the data and the measured energy dependence of the total cross section which follows more closely the energy dependence of the S_{11} resonance contribution than those of the other current contributions. The dominance of the S_{11} resonance in the $pp \rightarrow pp\eta'$ reaction potentially offers a unique opportunity to study the excitation mechanism of this resonance in $NN \rightarrow NN\eta'$, similar to the situation encountered in the case of η meson production [11], where the excitation of the $S_{11}(1535)$ resonance is the dominant reaction mechanism. In this connection, whether or not the S_{11} resonance also dominates in the $pn \rightarrow pn\eta'$ and/or $pn \rightarrow dn\eta'$ reactions remains still to be seen.

4 Analysis of the (preliminary) CLAS data on $\gamma p \rightarrow p\eta'$ reaction

Our model results for the (preliminary) CLAS data on η' photoproduction [12] are shown in Fig. 4a. First of all, compared to the SAPHIR data [8] analyzed in Section 2, the new CLAS data are much more accurate and, as such, may reveal features that were not seen in the analysis of the SAPHIR data. In Fig. 4a, different curves correspond to different sets of fit parameters which yield comparable χ^2 . Unlike the case of the SAPHIR data, here one requires, not only the spin-1/2 resonances, but also the spin-3/2 resonances in order to reproduce the data. We found that the required spin-1/2 and -3/2 resonances are consistent with those quoted by the PDG [13].

Although the different parameter sets yield practically the same differential cross sections, except for very forward and backward angles where no data exist, the corresponding dynamical content is very different from each other over the entire angular range. This shows in particular that cross sections alone are unable to fix the resonance parameters unambiguously, and that more exclusive observables, such as the beam and target asymmetries, are necessary in order to extract information on nucleon resonances.

Our predictions for the total cross section, as displayed in Fig. 4b, have been obtained by integrating the differential cross section results of Fig. 4a. A common feature present in all of these results is the bump structure around $W = 2.09$ GeV. If this is confirmed, the $D_{13}(2080)$ (and possibly $P_{11}(2100)$) resonance is likely to be responsible for the structure. The PDG [13] quotes $D_{13}(2080)$ and $P_{13}(2100)$ as two and one star resonances, respectively. Another feature

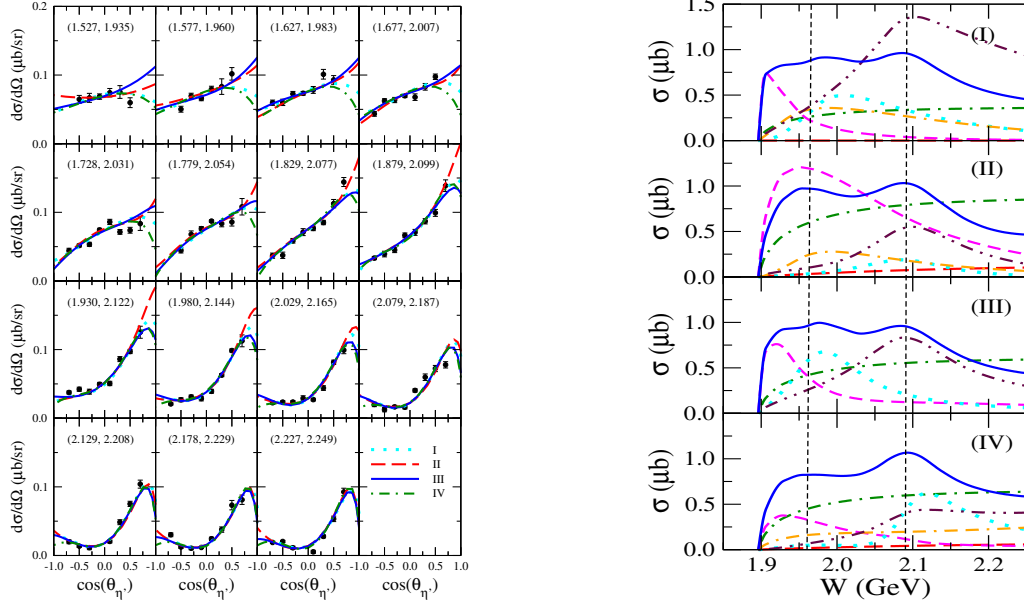


Fig. 4. Left figure (a): Same as Fig. 2 for the CLAS data [12]. The curves correspond to different fit results which yield comparable χ^2 to each other. The numbers (T_γ, W) in parentheses are the incident photon energy T_γ and the corresponding s -channel energy $W = \sqrt{s}$, respectively, in GeV. Right figure (b): Total cross section for $\gamma p \rightarrow p\eta'$ as a function of W . As indicated in the legend, the panels correspond to the fit results shown in the left figure. The overall total cross sections (solid lines) are broken down according to their dynamical contributions. The dash-dotted curves correspond to the mesonic current contribution; the dashed curves to the S_{11} resonance current and the dotted curves to the P_{11} resonance. The dot-double-dashed curves correspond to the P_{13} resonance current while the dash-double-dotted curves show the D_{13} resonance contribution. The nucleonic current contribution (long-dashed curves) are negligible and cannot be seen on the present scale. The two dashed vertical lines are placed to guide the eye through the two bump positions in all panels.

we see in Fig. 4b is the sharp rise of the total cross section near threshold which is caused by the S_{11} resonance.

Contrary to the expectation in Section 2, the $NN\eta'$ coupling constant cannot be determined even with the high-precision CLAS data. The reason is that even at higher energies, the resonance contribution may be large, especially, that of the D_{13} resonance. In fact, two of the results shown in Fig. 4b correspond to practically vanishing $g_{NN\eta'}$. However, we are able to give a more stringent upper limit of $g_{NN\eta'} < 2$. In order to pin down this coupling constant, one needs to either have more exclusive data than the cross section or go beyond the resonance energy region.

5 Summary

The study of η' production processes is still in its early stage of development. Our study reveals that in order to extract relevant physics, one needs more exclusive data than the cross sections.

In addition, measurements of η' production using the neutron/deuteron target are also required, especially, in $NN \rightarrow NN\eta'$ reactions, in order to learn about the resonance excitation mechanisms which is not possible in more basic processes such as $\gamma N \rightarrow N\eta'$. On the other hand, our theoretical model also needs to be improved; in particular, coupled channel effects should be investigated. In this connection, unfortunately, there is no realistic model for the $N\eta'$ final state interaction available at present.

Acknowledgement: This work is partly supported by the COSY Grant No. 41445282 (COSY-58).

References

- [1] J. Ashman et al.: *Phys. Lett. B* **206** (1988) 364
- [2] G. M. Shore, G. Veneziano: *Nucl. Phys. B* **381** (1992) 23
- [3] K. Nakayama, H. Haberzettl: *Phys. Rev. C* **69** (2004) 065212 ; nucl-th/0507044
- [4] Q. Zhao: *Phys. Rev. C* **63** (2001) 035205
- [5] W. T. Chiang et al.: *Phys. Rev. C* **68** (2003) 045202
- [6] A. Sibirtsev, Ch. Elster, S. Krewald, J. Speth: AIP Conf.Proc.**717** (2004) 837; nucl-th/0303044
- [7] B. Borasoy: *Eur. Phys. J. A* **9** (2000) 95
- [8] R. Plötzke et al.: *Phys. Lett. B* **444** (1998) 555
- [9] F. Hibou et al.: *Phys. Lett. B* **438** (1998) 41 ; F. Balestra et al.: *Phys. Lett. B* **491** (2000) 29
- [10] P. Moskal et al.: *Phys. Rev. Lett.* **80** (1998) 3202 ; P. Moskal et al.: *Phys. Lett. B* **474** (2000) 416 ; P. Moskal et al.: *ibid.* **482** (2000) 356 ; A. Khoukaz et al.: *Eur. Phys. J. A.* **20** (2004) 345
- [11] K. Nakayama, J. Speth, T.-S. H. Lee: *Phys. Rev. C* **65** (2002) 045210 ; K. Nakayama et al.: *ibid.* **68** (2003) 045201
- [12] M. Dugger and B. Ritchie: *private communication*
- [13] S. Eidelman et al.: *Phys. Lett. B* **592** (2004) 1